Arch Bridges
ARCH´04
P. Roca and E. Oñate (Eds)

TRANSVERSE STRENGTH OF A MODEL MASONRY ARCH BRIDGE

Thomas E. Boothby[*], Ece Erdogmus[*] and Yurianto Yurianto[†]

[*] Department of Architectural Engineering
The Pennsylvania State University
104 Engineering Unit A, University Park, PA 16803 USA
e-mail: tebarc@engr.psu.edu

[†] Engineered Framing Systems, Inc.
8950 Route 108, Suite 228 Columbia, MD 21045 USA
e-mail: yy@engframesys.com

Key words: experiment, spandrel wall, transverse strength

Abstract. *It has recently been noted that the capacity of an arch bridge perpendicular to the span direction is at least as important as the capacity of the arch to span between abutments and that a large number of recent failures of masonry arch bridges have been the result of deficient spandrel wall capacity. In this study, a 1.5 meter span brick masonry arch bridge has been constructed and subjected to testing under a concentrated load adjacent to one of the spandrel walls. In this testing program, the bridge failed by collapse of the spandrel wall at a load of approximately 132 kN, while the arch barrel remained undamaged. An analytical model of the bridge has been developed using a commercially available three-dimensional non-linear finite element computer program. The analytical model accurately predicts the pattern of cracks preceding the failure of the structure and the eventual failure mode, although it overestimates the collapse load by approximately 10%. The model also achieves acceptable predictions of the deflections of the arch barrel and spandrel wall, and correctly predicts order of magnitude and trends in the strains of the brick masonry arch bridge system.*

—

1 INTRODUCTION

Although the literature on masonry arch bridges includes several series of ultimate strength tests of masonry arch bridges under controlled laboratory conditions[i-v] and in the field[vi-ix], all of these tests are configured to verify the capacity of the arch barrel in the span direction. However, experience with these bridges and recent analytical results[x] indicate that the capacity of the bridge perpendicular to the span direction is at least of equal importance. One recent work has addressed this issue, both by identifying structures that have failed due to transverse effects, and introducing a method for the determination of the propensity of a bridge to fail due to transverse effects[xi]. All previous large scale tests of masonry arch bridges have the objective of verifying the bridge capacity in the span direction and comparison of this capacity to the results of a two-dimensional analysis of a unit width of arch. As a result, in these testing programs, the load to is applied the surface of the bridge as a line load across the full width of the bridge using a spreader beam. In a single instance, at Strathmashie[vii], a bridge failed due to a blow-out of the spandrel wall, which failure has been reproduced analytically[x]. Having recognized the importance of this failure mode for masonry bridges, it is considered important to set up a large-scale experiment with the express purpose of replicating the failure of a spandrel wall, both in an experimental prototype and in a parallel analytical model. To this end, a masonry bridge model has been constructed and tested and an analytical model, based on the findings of Fanning and Boothby[xii], was developed, calibrated, and compared to the experimental results. The following paper is a discussion of this research program.

2. EXPERIMENTAL PROCEDURE

The experimental prototype described in this paper is an approximately half-scale model masonry arch bridge, located at the Pennsylvania Transportation Institute Test Track, Benner Twp, Pennsylvania. This bridge was built in 1996 by a professional mason from 200 mm common extruded and wirecut solid clay bricks laid up in a common bond pattern and bedded in ASTM C270 Type O mortar. A fine, non-cohesive soil was used for the fill. Coarse granular material (Penn DOT Class 2A sub base) was used for model bridge pavement to avoid premature soil failure due to applied bearing pressure. The model bridge total height was 1.8 meters and the total length was 4 meters. The total width was 1.5 meters and the clear width of the fill was 1.1 meter. A reinforced concrete slab 30 centimeters thick formed the base of this bridge. The intrados radius of the arch was 75 centimeters. The vault thickness was 20 centimeters. The clear span of the arch was 1.5 meters. The bridge was filled to a height of 1.675 m, including a 25cm thick layer of compacted base course material at the top of the fill. Figure 1 shows the completed bridge ready for testing. Figure 2 shows the dimensions of the bridge and the location of the bearing plate for load application.

During construction, the soil was deposited in 10 cm lifts and compacted, using a vibrating plate compactor, to at least 85% of maximum density by the Standard Proctor Test. 2×6 dimension lumber was applied to the ends from the bottom to the top of the fill. 4×4 timber reinforcing ribs were applied at the bottom, middle and top of the end restraint. Each

of the 4×4's was tied with 12 mm diameter steel cables, offset 50 mm from the spandrel wall to allow lateral deflection of the spandrel wall.

Figure 1: Model Bridge Prepared for Testing.

Several prisms were made from same masonry as the model, at the time the model was built. These prisms were tested by ASTM C1314 to obtain masonry compressive and tensile strength. A laser extensometer was also used to measure the strain of the masonry over a gauge length from center to center of the bricks. LVDT's were placed at both sides of the prism to measure any rotation in the prisms, in order to account for eccentric load in the test. Static compressive load was applied using a manually loaded hydraulic cylinder. Hydraulic pressure was read from a digital indicator attached to a pressure cell. All the prisms failed by developing vertical cracks at the middle of each side until one of the prism sides crushed. From the test results for the three prisms, an average compressive strength of 25 MPa and an average modulus of elasticity of 10 GPa were found. The masonry flexural tensile strength was obtained by using ASTM C1072 (Bond Wrench Test). Two prisms with five joints in each prism were tested. All the joints failed by rupture of the mortar without loss of bond between the mortar and the masonry units. The average masonry tensile strength obtained from these tests for the bridge model was 2.38 MPa.

The soil of the model was tested using a direct shear test to determine the soil angle of internal friction by plotting shear stress vs. normal stress. The horizontal load or shear load applied to the specimen was measured by a proving ring and applied by a motor and gear arrangement. The vertical load or normal load, N, was applied to the sample via a yoke and

weights. The shear stress and normal stress were determined by dividing the shear force and the normal force by the effective area of shear box. From two points of the soil shear test data, the internal friction angle of the soil was found to be 25º.

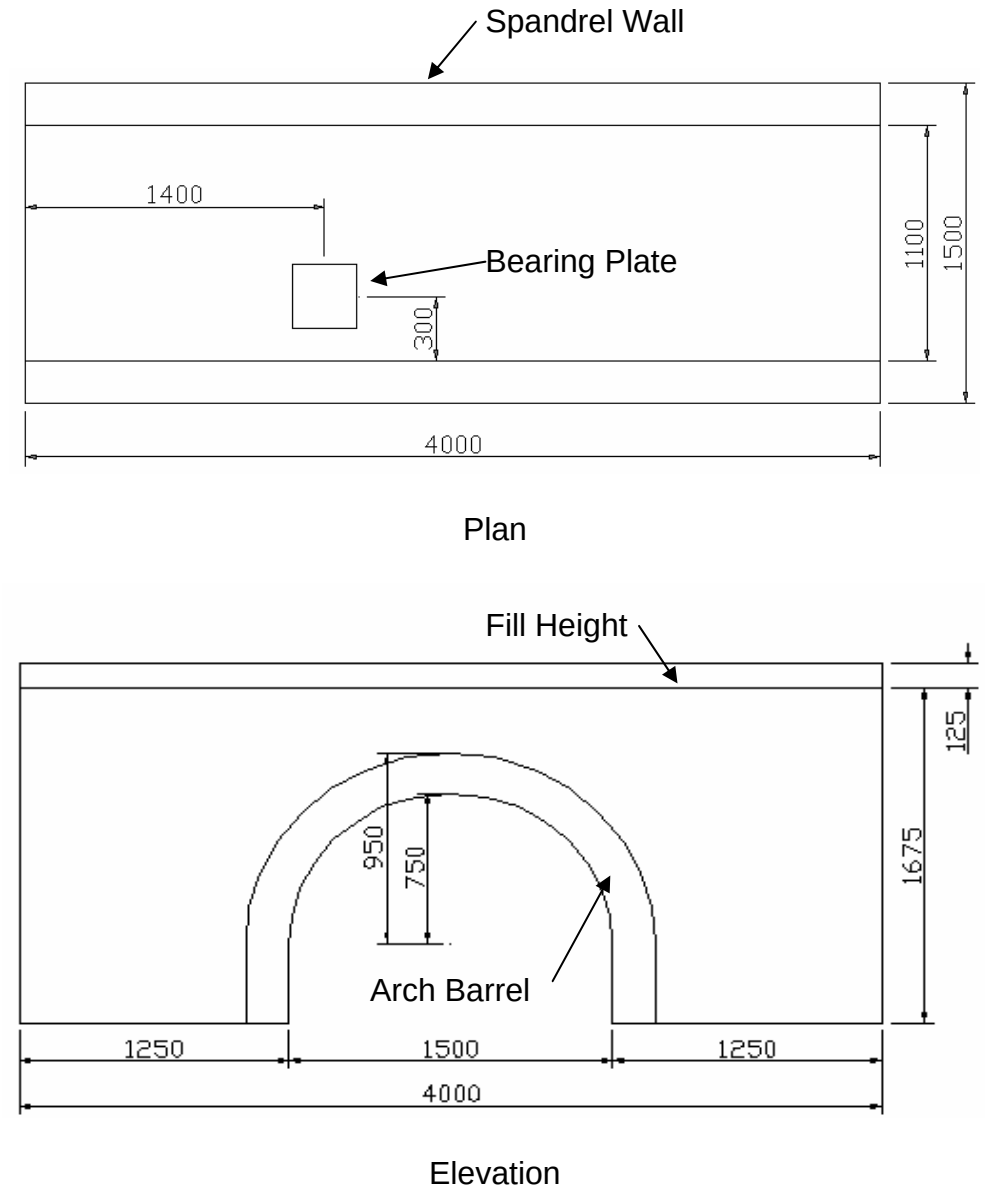

Figure 2: Dimensions of Model Bridge

The model bridge was loaded at the quarter span using a hydraulic loading jack on the top of 300 × 300 × 50 mm bearing plate. The displacements and strains of the spandrel wall and arch barrel were measured using LVDT's and strain gages. The LVDT's measured the vertical displacement under the arch barrel below the crown and below the loading location. Bonded electrical resistance strain gages were placed at the inner surface of the arch barrel, inner surface of the parapet, and below the arch barrel. All of the instrument data were recorded using a PC-based automatic data acquisition system.

3 MODELING

The model used for this structure is a three-dimensional, non-linear finite element model, using the computer program ANSYS 5.7[xiii]. The development of this procedure for modeling masonry arch bridges, and its validation by testing at service loads is described in detail in Fanning and Boothby[xii]. The masonry material of the bridge is modeled using SOLID65 three-dimensional eight-noded isoparametric elements and linearly elastic material properties. SOLID65 allows the formation of cracks perpendicular to the direction of any principal stress that exceeds the tensile strength of the masonry material. Values of masonry tensile and compressive strength obtained from the prism test results are used in the model. Examination of the bridge after testing revealed that, in spite of excellent flexural bond within the arch barrel and spandrel wall, the joint between the arch barrel and spandrel wall had very poor bond. This condition, which was probably due to insufficient wetting of the bricks at the interface when the spandrel wall built over the completed arch barrel, is apparent in the discussion of the results of the testing program. To replicate this condition in the finite element model, a tensile strength of 0.1 MPa is used for the row of elements along this interface.

The fill is modeled with a linearly elastic constitutive law. Linear elastic material parameters, modulus of elasticity of 5.6 MPa, Poisson's ratio of 0.37, and density of 2200 kg/m^3 are used for the fill material. The material properties for the fill are based on the findings of Fanning and Boothby (2001) on the modeling of masonry arch bridges. To allow movement or sliding of the fill material relative to the arch barrel and the spandrel walls without generating significant tensile stresses between fill and masonry material, the TARGE170 and CONTA173 element types are used as frictional contact surfaces. TARGE170 is used for three-dimensional target surfaces associated with a contact element, the CONTA173 element. The contact and target surface elements have the same geometric characteristics as the solid face that they are connected to. Using these contact pairs, compression forces from the passive soil pressure are fully transferred to the masonry, and tension forces cannot be transferred. Sliding friction, using a friction coefficient of 0.4, is also modeled by this contact pair. The pavement has higher stiffness than the remainder of the fill. Moreover, the addition of stiffer soil elements on the top prevents premature soil failure due to concentrated forces. Pavement elements are used to prevent early soil failure in the analytical model.

In the numerical model, the ends of the fill element nodes are restrained in the longitudinal direction while the base element nodes are restrained in the vertical direction. The end spandrel wall nodes are unrestrained. At the base of the spandrel wall, the nodes are restrained in the transverse and vertical directions. At the base of the arch barrel, the nodes are restrained in the longitudinal and vertical directions.

The model is meshed with a hexahedral element shape. The total length of the model is 4000 mm. In the longitudinal direction, the model is divided into 40 segments. The total height of the spandrel wall is 1800 mm and in the vertical direction, the model is divided into 18 segments. The thickness of the arch barrel and the spandrel wall are set to have 3 rows of elements. The 1100 mm width of the bridge is divided into 11 elements

Gravity load due to self-weight is first applied until the solution converges. After the solution under gravity load has converged, the model is loaded with a static pressure load on a 300×300 millimeter bearing area at the quarter span to simulate the hydraulic jack load applied to the bearing plate. The load is applied in 0.9 kN increments up to the experimental peak load. Nodal displacements at the LVDT locations in the experiment are recorded at each substep.

EXPERIMENTAL RESULTS

The bridge was tested on December 2, 2001. In the first test (Test #1), the experimental bridge was loaded slowly until the load reached 1.47 MPa bearing pressure on the full surface of the plate, or 132 kN force. At this point, the bridge had reached its capacity, and the testing was stopped. Following this, at a load level of 39 kN, the spandrel wall developed a vertical flexural crack, directly above the crown of the arch barrel, on the loaded side. This event was accompanied by a drop in the stiffness of the response of the spandrel wall, on the loading side (LVDT's 1 and 2) only. At approximately 70 kN, the spandrel wall began to rotate freely, without any increase in the load, most probably indicating the propagation of a crack through the entire thickness of the spandrel wall. After reaching a limit on the rotation of the wall, the wall stabilized and allowed further loading, although with a sharply reduced stiffness, until the maximum load of 132 kN is reached. Although 132 kN is the maximum load from this test, it cannot be called the 'ultimate load' on the model bridge, because the load was intentionally removed after reaching 132 kN. However, due to the damage to the bridge, it was not possible to exceed this load during subsequent testing of the structure. The maximum displacement recorded at LVDT 1 was 850 μm, with a residual displacement of approximately 450 μm, while at LVDT 2, the maximum displacement was 270 μm, and the residual was 225 μm. The arch barrel itself sustained no visible damage during the testing program. The response of all of the LVDT's located under the arch barrel shows a decrease in stiffness at 22 kN, on formation of the first crack, and a linear response thereafter, for both loading and unloading. The maximum displacement of the arch barrel recorded, at the quarter point under the load (LVDT 7), was 104 μm. Although small (approximately 20 μm) residual

displacements are apparent in LVDT's 6 and 7, the crown, which underwent displacements of approximately 50 μm, shows no measurable residual displacements. Moreover, because the arch barrel separated from the spandrel wall at a low load level, the spandrel wall did not contribute appreciable stiffness to the edge of the arch barrel, and displacements were roughly uniform across the width of the arch barrel, both at the quarter point and at midspan. Detailed displacement output from the LVDT's is shown and discussed in the following section on modeling results for the bridge.

After the peak load was reached, the structure was unloaded, and then re-loaded in Test #2. During this test, the load reached a peak of 130 kN, beyond which the load on the cylinder decreased while the piston continued to extend. During this test, an additional 540 μm displacement was recorded at LVDT 1, with an additional increment of residual displacement of 170 μm. LVDT 4, on the spandrel wall opposite the loading, did not record significant displacements. All of the LVDT's in the arch barrel, 5-7, 8, 10, and 12 recorded practically identical results to the results of Test #1. During further repetitions of the load application, the spandrel wall initiated sliding at the interface with the arch barrel at a load of 115 kN. This sliding was on the order of several millimeters.

The photographs taken after the conclusion of the testing program show the final condition of the spandrel wall on the loading side. At the joint between the arch barrel and spandrel wall, over 10 mm translation of the entire spandrel wall with respect to the plane of the arch barrel was observed.

Analytical Results and Comparison to Experimental Results

The load program used in the finite element analysis is a simulation of Test #1. The first cracks at both joints between arch barrel and spandrel develop simultaneously when the load reaches 36 kN. The cracks continue to grow at the joints as more load is applied. The joint cracks at the loaded side grow more rapidly than the cracks the side away from the load. The arch ring joint with the base cracks at 76 kN. The spandrel wall at the loaded side begins to shift laterally from the arch ring as the cracks from the middle and base of the arch ring meet at 118 kN. The parapet over the crown cracks at a load of 122 kN. Spandrel wall collapse is induced by the separation of the arch ring and the crack at the parapet over the crown of the arch. The soil pressure pushes the spandrel wall at the side until it become completely detached from the bridge at a load of 146 kN. The patterns of cracks induced in the bridge during the experiment, and the cracks developed in the model are shown in Figure 3. Figure 4 shows the results from the analysis for the row of LVDT's at the crown of the arch barrel, along with experimental results from Test #1 for LVDT 10 and 12. LVDT 10 was located at the mid-width and LVDT 12 under the spandrel wall on the loaded side. The deflections at LVDT 10 and LVDT 12 are very well predicted by the analytical model, although the analytical model predicts inelastic behavior at high load levels, which was not encountered in the experiment.

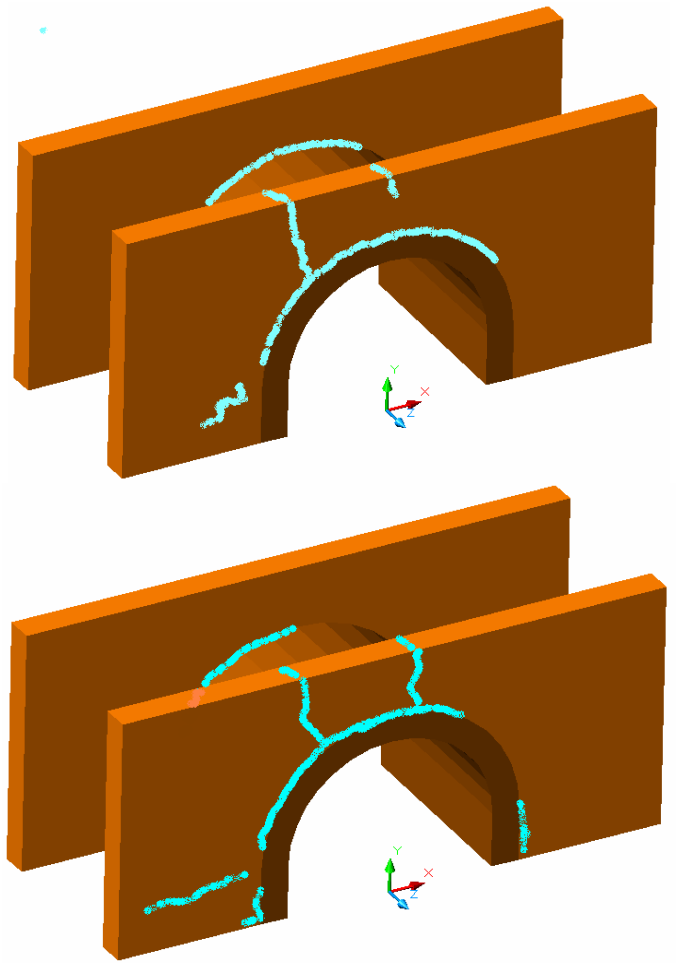

Figure 3: Crack Patterns of Model Bridge: Experimental Above, and Analytical Below

Figure 5 shows the results from the analysis for the location of LVDT's #1 and #2, measuring lateral displacements at the spandrel wall on the loaded side, superimposed on a diagram of the actual displacements of LVDT's 1 and 2 The significant events in the failure of the analytical model are annotated in the figure. LVDT 2 is at the top of the spandrel wall close to the loading point. The analytical model estimates the deflections at this point quite accurately, although the softening influence following crack development is underestimated by the model. The analytical model correctly predicts that the spandrel wall slides at a high load level but slightly overestimates the load at which this event occurs. The analytical model also overestimates the ultimate load by approximately 10%. The analytical model generally anticipates greater displacements at the corner of the spandrel wall where LVDT #1 was positioned, although it predicts the trend and order of magnitude of these displacements reasonably well.

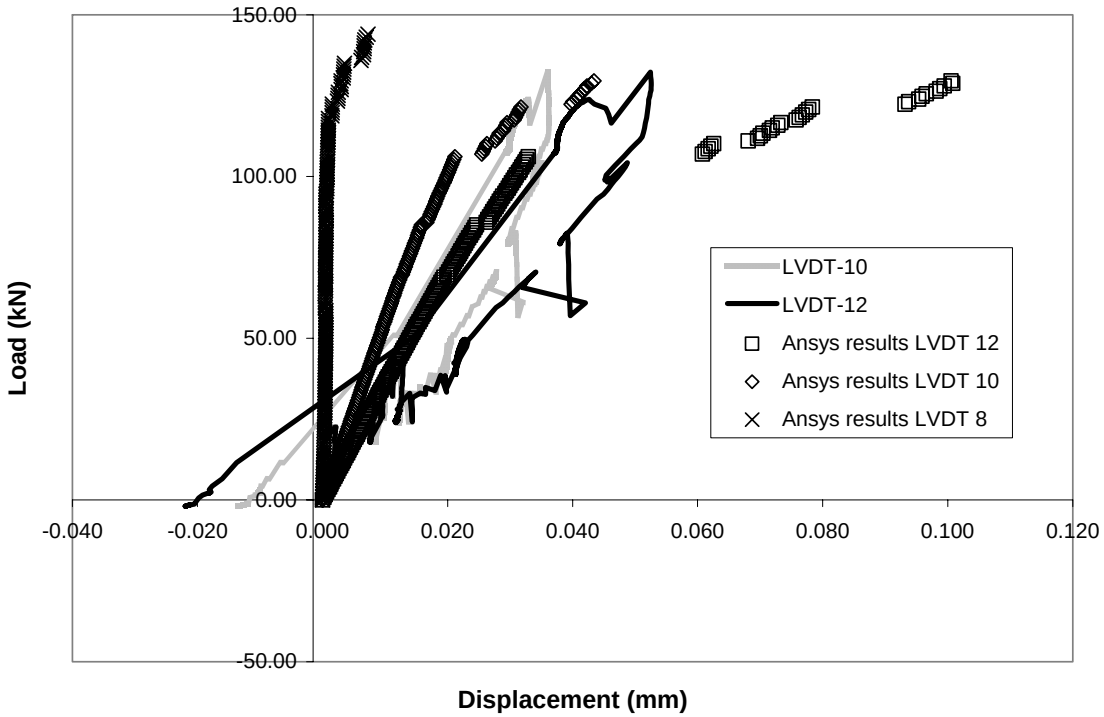

Figure 4: Displacement Results for Arch Barrel

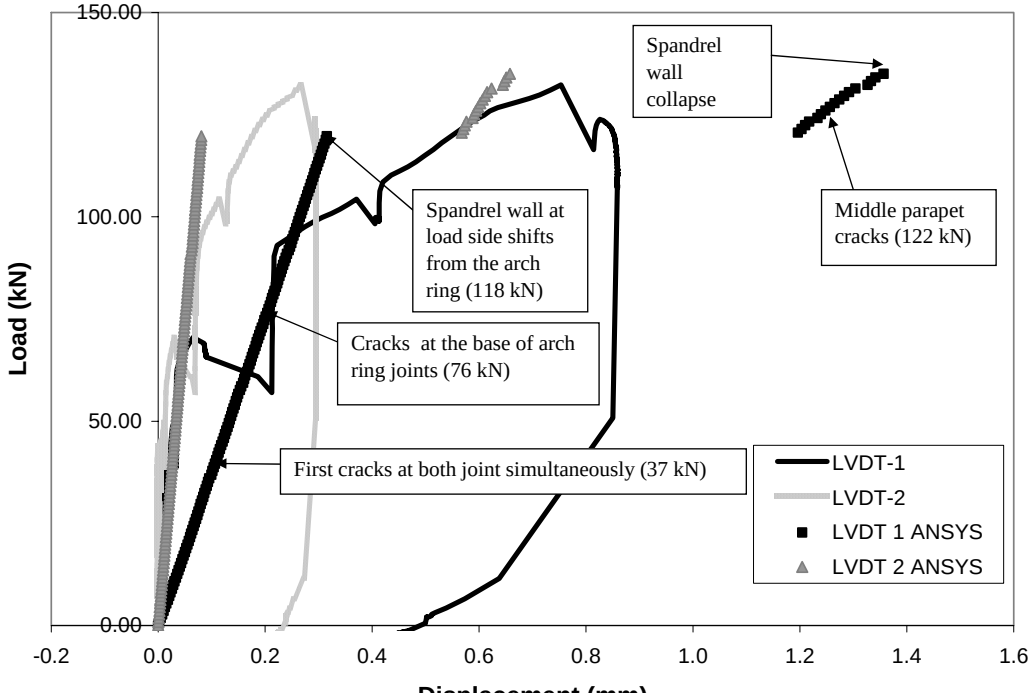

Figure 5: Displacement Results for Spandrel Wall

CONCLUSIONS

This research has provided a clear demonstration of the importance of transverse effects in the assessment of masonry arch bridges, through the completion of a test of a model masonry arch bridge, through the subsequent analysis of the experimental results, and through the development of a three-dimensional non-linear finite element model capable of replicating the failure mode and failure load of the structure. The failure of the model bridge examined in this work is entirely due to collapse of spandrel wall. This collapse, which is similar to conditions observed in actual bridges, results from transverse soil pressure in the fill: the arch barrel itself sustained no damage and was subjected to very small strains and displacements. Other findings of this research are the demonstration of the applicability of the three-dimensional non-linear finite element analysis method to the assessment of in-service bridges by evaluating permissible applied truck loads and replicating crack patterns or other visible damage. The following are the detailed conclusions the study, along with some recommendations for further research.

The experimental bridge failed due to transverse deformations. Although the first cracks occurred at the joints between the arch barrel and the spandrel wall, there was no local failure or hinge mechanism observed in the arch barrel. The first cracks formed prematurely because of the high intensity of load applied at the arch barrel, which caused the arch barrel to be deflected vertically downwards to the load direction. This finding is substantiated by the experimental strain values at the arch barrel located below the load, which are high compared to the analytical strain results. After the cracks were fully developed along the joints, internal soil pressure on the spandrel wall caused the spandrel wall to shift from the arch barrel at the same time the parapet cracked. The high fill depth at each side of the model bridge produced higher lateral soil pressure to the end spandrel walls. The model bridge eventually collapsed due to overturning and sliding of the spandrel wall.

The three-dimensional, non-linear finite element bridge model developed in this study accurately simulated the behavior of the experimental bridge. Under the same type of geometry, material properties and loading conditions, the finite element model produced similar failures. The finite element model analysis shows that the first cracks occur prematurely at the same location as the experimental bridge. The cracks at joints between the arch barrel and the spandrel wall grow more slowly compared to the experimental bridge. This may have occurred because the finite element model had more idealized end boundary behavior. Both the experimental and finite element model behave with similar global stiffness after the spandrel wall shifts from the arch barrel. The crack patterns at failure produced in the finite element analysis are similar to the actual crack patterns that occurred. The greatest deflection of the analytical model was at the corner top of the end spandrel wall, which was the same as in the experimental bridge. The spandrel wall collapsed by overturning due to the internal soil pressure. All of this evidence shows that three-dimensional, non-linear finite element analysis is capable of reproducing or predicting

experimental results for masonry arch bridges, where the transverse failure mode governs over the span effect failure mode.

The SOLID65 element type was proven adequate to replicate the crack pattern of the experimental bridge. Using a lower strength material at the joint of the masonry analytical model has successfully predicted premature cracks.

The boundary conditions directly influence the results of the analytical bridge model. In the finite element analysis model, the boundary conditions are assumed fixed in the directions where the nodes are restrained. The base of the experimental model bridge is made from a thick concrete slab, which imposed fixed boundary conditions in the vertical direction on the base. However, the ends for the fill of the bridge, made of solid sawn lumber, are tied at the top, middle and bottom elevations with cables. On the completion of the tests, the internal soil pressure induced by the test load caused some displacement of the end restraints. This may have led to different behavior between the experimental model and the finite element analysis model.

REFERENCES

[i] Melbourne, C., Begimil, M. and Gilbert, M. "The load test to collapse of a five meter span brickwork arch bridge with tied spandrel walls." *Arch Bridges*, Thomas Telford, London, 509-517, 1995

[ii] Royles, .R. and Hendry, A.W. Model tests on masonry arches. *Proceedings of the Institution of Civil Engineers, Part 2*, 91(6):299-321, 1991

[iii] Melbourne C. and Wagstaff, D. Load tests to collapse of three large scale multispan brickwork arch bridges. *Second International Confernece on Bridge Management.* University of Surrey, 1993

[v] Begimgil M. "Behavior of restrained 1.25m span model masonry arch bridge," *Arch bridges*, Thomas Telford, London, 321-325, 1995

[iv] Melbourne, C. and Gilbert, M. The behaviour of multi-ring brickwork arch bridges containing ring separation. *Third International Masonry Conference.* The British Masonry Society, London, 1992

[vi] Page, J. *Load tests to collapse on two arch bridges at Torksey and Shinafoot.* Transport and Road Research Laboratory Research Report 159. TRL, Crowthorne, UK, 1988

[vii] Page, J. *Load tests to collapse on two arch bridges at Strathmashie and Barlae.* Transport and Road Research Laboratory Research Report 201. TRL, Crowthorne, UK, 1989

[viii] Page, J. *Masonry Arch Bridges.* HMSO, London, 1993

[ix] Page, J. *Load tests to collapse on two arch bridges at Preston, Shropshire and Prestwood, Staffordshire.* Transport and Road Research Laboratory Research Report 157. TRL, Crowthorne, UK, 1987

[x] Boothby, T.E. and Roberts, B.J. Transverse behaviour of masonry arch bridges. *The Structural Engineer,* 79(9):21-26, 1 May 2001

[xi] Erdogmus, E. and Boothby, T.E. Strength of spandrel walls in masonry arch bridges, to appear *Journal of the Transportation Research Board,* 2004

[xii] Fanning, P.J., and Boothby, T.E. Three Dimensional Modeling And Full-Scale Testing of Masonry Arch Bridges, *Computers and Structures, Vol 79, 2645-2662,* 2001

[xiii] ANSYS, Inc. "ANSYS Manual, Release 5.7." SAS IP,Inc, 2001